

Determination of the first-generation quark couplings at the Z -pole

K. Mękała,^{a,b,1} D. Jeans,^c J. Reuter,^b J. Tian,^d and A.F. Żarnecki^a

^a*Faculty of Physics, University of Warsaw, Pasteura 5, 02-093 Warsaw, Poland*

^b*Deutsches Elektronen-Synchrotron DESY, Notkestr. 85, 22607 Hamburg, Germany*

^c*KEK, 1-1 Oho Tsukuba, Ibaraki 305-0801, Japan*

^d*International Center for Elementary Particle Physics ICEPP, University of Tokyo, 7-3-1 Hongo, Bunkyo-ku, Tokyo 113-0033, Japan*

E-mail: k.mekala@uw.edu.pl, daniel.jeans@kek.jp,
juergen.reuter@desy.de, tian@icepp.s.u-tokyo.ac.jp,
filip.zarnecki@fuw.edu.pl

ABSTRACT: Electroweak Precision Measurements are stringent tests of the Standard Model and sensitive probes to New Physics. Accurate studies of the Z -boson couplings to the first-generation quarks, which are currently constrained from LEP data to a few percent, could reveal potential discrepancies from the theory predictions. Future e^+e^- colliders running at the Z -pole would be an excellent tool for an analysis based on a comparison of radiative and non-radiative Z boson decays. In this paper, we present a method to extract the values of the Z couplings to light quarks and discuss the uncertainty of the measurement, including contributions from various systematic effects. We show that systematic uncertainty in the heavy-flavour tagging performance is the key factor in the analysis and reducing it to a sub-permille level might be crucial to fully profit from the high luminosity of future e^+e^- machines. The measurement could improve the LEP results by at least an order of magnitude.

¹Corresponding author.

Contents

1	Motivation	2
2	Outline of the measurement	3
3	Simulation of events	4
4	Analysis procedure and results	7
4.1	Event reconstruction	7
4.2	2-flavour fit	8
4.3	5-flavour fit	10
4.4	Discussion of systematic uncertainties	11
4.5	Discussion of correlations in the measurement	12
5	Conclusions and outlook	14
A	Coupling fit framework	16
A.1	Fit with statistical uncertainties only	16
A.2	Including systematic uncertainties	18

1 Motivation

The Standard Model (SM) of particle physics is the best theory to describe fundamental interactions at excellent precision. Although several experiments, including cosmological observations, point to the existence of exotic components of matter building the Universe, to date no single particle has been found Beyond the Standard Model (BSM). To reveal the unknown, the particle physics community agrees on the necessity of exploring new directions, after completing the Large Hadron Collider (LHC) programme, by building an e^+e^- Higgs factory, as expressed in the 2020 Update of the European Strategy for Particle Physics [1] and the P5 Report in the US [2]. Not only would such a collider improve the measurement of the properties of the Higgs boson, but it would also allow for direct searches of New Physics, as well as deliver the most precise constraints on the parameters in the electroweak sector. The latter is perceived as the main reason behind starting the operation of the new facility at the Z -pole, collecting unprecedented statistics of Z bosons in a clean collision environment. The Z -pole runs are currently considered for most facilities: CEPC [3, 4], FCC-ee [5], ILC [6–8], and LCF [9, 10], differing in achievable luminosities ($10^2 - 10^5 \text{ fb}^{-1}$). The measurement discussed in this paper is not sensitive to beam polarisation assumed for linear machines, and we will not consider it in the following.

Among others, the huge collected statistics of Z bosons could be used to measure its electroweak couplings to quarks. The LEP experiments achieved per-mille precision in constraining the partial width of the Z -boson decaying into $b\bar{b}$ pairs and percent precision for $c\bar{c}$ pairs [11]. Improvements in detector technologies and heavy-quark tagging algorithms¹, are expected to significantly improve these results at future colliders (see e.g. [12–19]). However, due to the lack of efficient tagging algorithms, direct measurements for light quarks are challenging, and an alternative approach is required. Since the probability of photon emission is related to the electric charge of the particle, up-type quarks emit photons with much higher probability compared to down-type quarks. Conversely, down-type quarks dominate the non-radiative sample due to the larger value of the SM electroweak coupling. These observations can be leveraged to study the hadronic decays of the Z boson by simultaneously examining both radiative and non-radiative signatures, thereby disentangling their dependence on the value of the couplings. Similar measurements were taken at LEP [20–24] and yielded results of up to 3% uncertainty for d and 6% for u quarks. Our analysis aims to extend this work towards future colliders, taking into account modern experimental developments.

In this paper, we introduce the proposed method and examine its applicability to future e^+e^- colliders operating at the Z pole. The conceptual framework for the measurement is outlined in Section 2. Section 3 details our event-generation procedure and theoretical modelling. The subsequent Section 4 presents the analysis framework and the obtained results. Finally, we provide our conclusions and outlook in Section 5. Additional information on the employed statistical methods is provided in the Appendix A.

¹Throughout the paper, we will refer to the u and d quarks as “light” and to the others, including the s quark, as “heavy”.

2 Outline of the measurement

The concept of the measurement relies on the fact that up- and down-type quarks differ in electric charge and thus, their electromagnetic couplings are distinguishable. The coupling strength of the Z boson to a given fermion f is conventionally defined as

$$c_f = v_f^2 + a_f^2, \quad (2.1)$$

where v_f (a_f) is the vector (axial) coupling. In the SM, the couplings are expressed in terms of the third component of the fermion weak isospin ($I_{3,f}$) and its charge (Q_f):

$$v_f = 2I_{3,f} - 4Q_f \sin^2 \theta_W, \quad a_f = 2I_{3,f}, \quad (2.2)$$

where θ_W stands for the weak mixing angle. The total width of the Z boson to hadrons, Γ_{had} , is given at fixed order in α_s by [11, 21, 24]

$$\Gamma_{had} = N_c \frac{G_\mu M_Z^3}{24\pi\sqrt{2}} \left(1 + \frac{\alpha_s}{\pi} + \mathcal{O}(\alpha_s^2)\right) \sum_{q=u,d,s,c,b} c_q, \quad (2.3)$$

where N_c is the number of colours, G_μ is the Fermi constant, M_Z is the mass of the Z boson and c_q is the coupling to a given quark², respectively. The total width to radiative hadronic decays, $\Gamma_{had+\gamma}$, can be expressed at leading QED order as

$$\Gamma_{had+\gamma} = N_c \frac{G_\mu M_Z^3}{24\pi\sqrt{2}} f(y_{cut}) \frac{\alpha}{2\pi} \sum_q c_q Q_q^2, \quad (2.4)$$

where $f(y_{cut})$ is an acceptance factor depending on a parameter y_{cut} incorporating the isolation criteria for photons, α is the electromagnetic coupling constant and Q_q is the electric charge of the given quark. Since the electric charges of u -type and d -type quarks are different, the expressions for the radiative and the total hadronic widths include different coupling combinations, and the dependence on the couplings c_q can potentially be resolved.

Similarly, the hadronic cross section on the Z pole, $e^+e^- \rightarrow Z \rightarrow q\bar{q}$, $q = u, d, s, c, b$, can be expressed as

$$\sigma_{had} = \sum_q \sigma_q = \mathcal{C}_1 \cdot \sum_q c_q, \quad (2.5)$$

where \mathcal{C}_1 is a constant. The radiative hadronic cross section with exactly one photon identified in the final state (the one-photon inclusive cross section) can be parametrised as

$$\sigma_{had+\gamma} = \mathcal{C}_2 \cdot \sum_q c_q Q_q^2, \quad (2.6)$$

where \mathcal{C}_2 is another constant (for a given set of cuts and isolation criteria for photons). The values of \mathcal{C}_1 and \mathcal{C}_2 can be estimated from theoretical calculations and simulations.

In the simplest case, it suffices to identify light-quark events by excluding contributions from heavy-quark events through flavour tagging algorithms. Fitting the experimental data to theory predictions allows for the extraction of c_u and c_d using the well-established maximum likelihood method. More details on the generalised formalism including the impact of systematic uncertainties are given in Appendix A.

²From now on, we will always assume that the sum runs over five quark flavours.

3 Simulation of events

High accuracy of the measurement can only be achieved if experimental data is compared with realistic and precise Monte Carlo simulations. Although the process of $e^+e^- \rightarrow q\bar{q}$ is one of the simplest electroweak processes and thus often perceived as a benchmark point for event generators (cf. e.g. [25]), the reconstruction of isolated photons poses several challenges. A proper description of the process necessitates the full Matrix-Element (ME) generation of the measurable photons. However, soft and collinear photons must be technically generated using modelling methods, such as parton showers. Additionally, due to the background originating from hadron decays, hadronisation effects must also be incorporated. Thus, as a recipe, one can generate data samples using fixed-order ME calculations, with exclusive emissions of hard photons, and match them with initial-state radiation (ISR) structure functions and final-state radiation (FSR) showers, accounting for collinear and soft emissions, and hadronisation models.

A similar issue was investigated in [26] where dark-matter production detected in the mono-photon signature at lepton colliders was considered. A matching procedure for simulating photons using both ME calculations (for hard emissions) and ISR structure function (for soft emissions) was developed for WHIZARD [27, 28], a Monte Carlo generator incorporating many features suitable for future lepton colliders, including beam polarisation, beamstrahlung and ISR spectra. WHIZARD uses the colour-flow formalism for QCD partons [29]. For the purpose of this study, it is sufficient to consider the leading-order contributions in QCD and electroweak interactions, though WHIZARD is capable of automated NLO QCD+EW corrections [30]. As the processes simulated here are relatively simple, we do not have to make use of the extensive parallelisation capabilities of WHIZARD [31, 32]. The procedure of [26] was validated against KKMC [33, 34]. We follow and extend this approach to include effects occurring for hadronic final states. Thus, parton-level events are generated with WHIZARD, and PYTHIA 6 [35] is employed to simulate parton showers and hadronisation. A standard cut on the invariant mass of the parton-level hadronic system to be above 10 GeV was applied. It was verified that the obtained results do not differ qualitatively when using PYTHIA 8 [36].

The matching in [26] is based on two variables, q_- and q_+ , defined for each photon as:

$$q_- = \sqrt{4E_0E_\gamma} \sin \frac{\theta_\gamma}{2},$$

$$q_+ = \sqrt{4E_0E_\gamma} \cos \frac{\theta_\gamma}{2},$$

where E_0 is the nominal beam energy, E_γ is the energy of the emitted photon and θ_γ is its emission angle. The variable q_- (q_+) corresponds to the virtuality of an electron (positron) after a single photon emission. According to the procedure, all the photons with $q_\pm > q_{min}$ and $E_\gamma > E_{min}$ are generated in the fixed-order calculation picture, while all the *softer* emissions are modeled via the built-in ISR structure function handler for the ISR photons in WHIZARD.

The procedure of [26] was developed for chargeless particles in the final state (electrically neutral and colourless). Hadronic decays of the Z bosons require an extension of the

matching to include final-state QCD and QED showers. Thus, to separate *hard* and *soft* final-state radiation regimes, we use an additional criterion based on the invariant mass of the photon-quark pairs, $M_{\gamma q_{1,2}}$. A *hard* photon is defined as one fulfilling all the following criteria:

- $q_{\pm} > 0.5$ GeV,
- $E_{\gamma} > 0.5$ GeV,
- $M_{\gamma q_{1,2}} > 1$ GeV,

and is generated using fixed-order ME calculations. All remaining *soft* photons (those not meeting at least one of those criteria) are simulated via the internal structure function handler for ISR photons in WHIZARD and the PYTHIA parton shower for FSR. Events with at least one ISR or FSR photon passing the *hard* photon selection are rejected to avoid double counting.

We generated samples with 10 million events with 0 ME photons, 10 million events with 1 ME photon and 1 million events with 2 ME photons. Higher photon multiplicities have been neglected, as the cross section for the 2-ME-photon sample is already about 30 times smaller than that for the 1-ME-photon sample. The samples were then matched according to the procedure described above. Table 1 summarises the cross sections for each flavour for all the *unmatched* samples (with generator-level cuts applied only to ME photons, but not those modelled in showers) and the final matched sample. As expected, the cross section for the matched samples is consistent with the cross sections of the unmatched 0-ME-photon samples.

σ_q [fb]	d	u	s	c	b	total
0 γ unmat.	5.46e+06	4.28e+06	5.46e+06	4.28e+06	5.47e+06	2.49e+07
1 γ unmat.	3.63e+05	4.63e+05	3.63e+05	4.65e+05	3.64e+05	2.02e+06
2 γ unmat.	8.48e+03	2.19e+04	8.51e+03	2.19e+04	8.50e+03	6.92e+04
0+1+2 γ mat.	5.44e+06	4.34e+06	5.45e+06	4.33e+06	5.45e+06	2.50e+07

Table 1. Cross sections for each quark flavour for unmatched samples (generator-level cuts applied only to ME photons) and the final matched sample. Integration uncertainties are below 10^{-3} .

Figure 1 shows the fraction of rejected events in the matching procedure for the sample with no photons generated at the matrix-element level for different quark flavours, normalised to the cross section per flavour, for ISR and FSR. As expected, the rejection efficiency for the ISR does not depend on the quark flavour while the rejection efficiency for the FSR distinguishes up- and down-type quarks and differs by a factor of about four between the two cases, which corresponds to the difference in the quark charge squared.

To account for experimental effects, we simulated detector response in DELPHES 3.5 [37], using the ILCgen cards based on the performance of the ILD and SiD concepts [38, 39]. Although originating from linear-collider studies, ILD is currently also considered for circular colliders [25, 40].

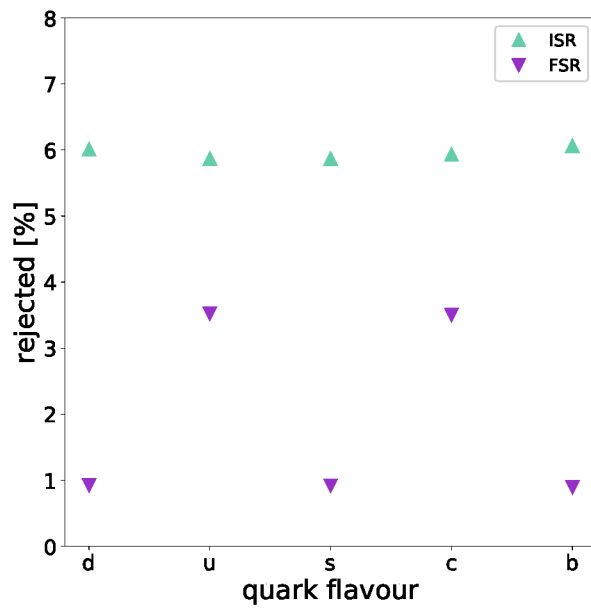


Figure 1. The fraction of events from the sample with no photons generated at the ME level rejected by the matching procedure for different quark flavours (normalised to the cross section per flavour) for ISR (aquamarine upwards) and FSR (purple downwards).

4 Analysis procedure and results

4.1 Event reconstruction

One of the advantages of the measurement at the Z -pole is the suppression of the ISR background contribution due to the small phase space for photon emissions. Nevertheless, background photons originating from hadronic decays must be considered in the analysis. Photon reconstruction criteria should be optimised at the experimental level to enhance the contribution from events with the actual hard emissions. We ignore other background channels to the inclusive sample of hadronic Z decays, as their impact is expected to be negligible.

At the ME level, we define the photon isolation parameter as

$$q^T = E_\gamma \sin \theta_{\gamma q_i}^{min}, \quad (4.1)$$

where E_γ is the photon energy and $\theta_{\gamma q_i}^{min}$ is the angle between the photon and the closest quark. The variable corresponds to the photon transverse momentum relative to the quark direction. The redefinition of the variable to the detector-level analysis is straightforward: the angle $\theta_{\gamma q_i}^{min}$ is replaced by $\theta_{\gamma j_i}^{min}$, the angle between the photon and the closest jet.

The Durham jet algorithm in the exclusive mode was used in DELPHES to cluster all final state objects into two jets. The photon isolation criteria were not applied in DELPHES, so all photons were included in the jet clustering. It allowed us to separate radiative event tagging from the standard reconstruction procedure and treat each photon equally, focusing on the analysis-specific approach³.

Figure 2 (left) shows the distribution of q^T for all reconstructed photons at the detector level. The number of events corresponds to a future e^+e^- collider collecting 100 fb^{-1} of unpolarised data and can be easily scaled for other luminosities. Only photons with an energy above 2 GeV and an absolute value of pseudorapidity below 2.5 were assumed to be measured. For low values of q^T , the total distribution is dominated by the 0-ME-photon sample (for which the reconstructed photons originate from hadronic decays, with 90% of the photons coming from π^0 decays, 6.4% from η decays and 0.9% coming from $\omega(782)$ decays), while for larger values the 1-ME-photon sample becomes dominant. The transition between the two regions occurs at about 10 GeV. For such values, the 1-ME-photon sample contains only hard photons, i.e. those generated at the ME level and not modelled in showers. Figure 2 (right plot) shows the *signal* efficiency (ratio of the accepted radiative events over all the radiative events) and purity (ratio of the accepted radiative events over all the accepted events) in the sensible range of possible values of y_{cut} . For the purpose of this study, we consider as signal only those events with exactly one hard tagged photon, i.e. for which $q^T > y_{cut}$. Events with one proper photon generated at the ME level become dominant for a cut value of about 7 GeV, for which about 10% of events are preserved.

³In this context, the physical interpretation of the q^T variable becomes somewhat vague, as including all photons in jets changes jet kinematics. We will, however, consistently follow our definition which remains comprehensive at the analysis level.

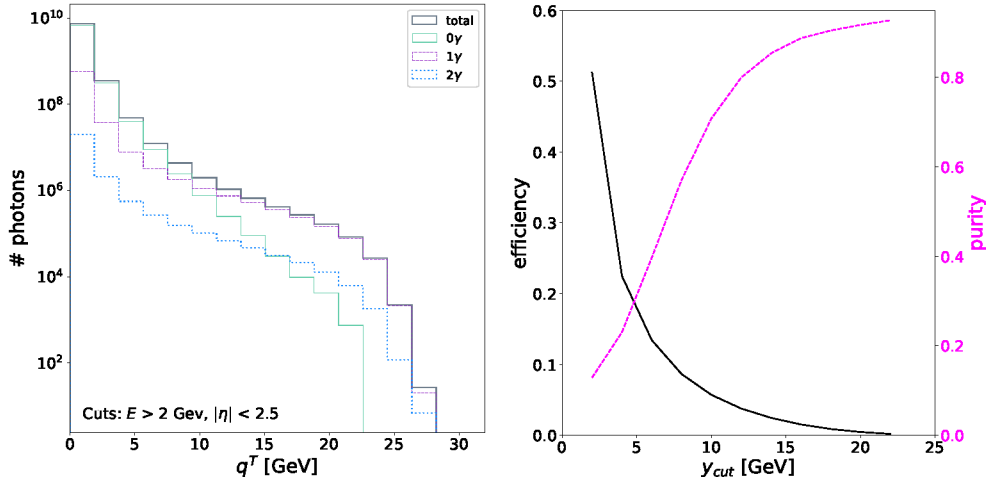


Figure 2. **Left:** the distribution of measurable photons (normalised to an integrated luminosity of 100 fb^{-1}) as a function of q^T . The thick gray line stands for the sum of all the samples, the solid aquamarine line for the 0-ME-photon sample, the purple dashed one for the 1-ME-photon sample and the blue dotted one – for the 2-ME-photon sample. Fast detector simulation is included in the results. **Right:** the signal efficiency (left axis, black solid line) and the signal purity (right axis, pink dashed line) for different values of y_{cut} , starting at a minimal value of 2 GeV considered in the study. Note that the distributions are defined at the event level, i.e. they relate to the number of those events in which exactly one photon was tagged.

4.2 2-flavour fit

In the next step, we used the statistical framework described in Appendix A. The quark flavour tagging efficiencies were adapted from [16] assuming that both jets are tagged independently and light quarks have exactly the same tagging probabilities⁴. Each jet was assigned one of the four available jet labels: “light jet”, “ s jet”, “ c jet”, or “ b jet”.

Firstly, we considered a sample of events with two tagged “light jets” only, i.e. we rejected all events in which at least one jet was not classified into the first category. We applied a transverse momentum cut $p_{j_i}^T > 10$ GeV and a pseudorapidity cut $|\eta_{j_i}| < 4$ on both jets. In this sample, we identified a subsample consisting of events with at least one photon tagged ($E_\gamma > 2$ GeV, $|\eta| < 2.5$). The numbers of events in the main inclusive sample (referred to as “hadronic” in the following) and its subsample (“radiative”) were used to fit the data and extract c_d and c_u using χ^2 minimisation. In our approach, the radiative subsample has not been removed from the hadronic sample; an alternative approach could be followed, namely removing the radiative events and changing the fit procedure accordingly, but it should not change the final results.

Subsequently, we studied the impact of systematic uncertainties, extending the fit procedure as described in Appendix A. We assumed that the measurement is affected by the following factors:

⁴The latter follows from the fact that the goal of our analysis is to separate the light-quark couplings using photon radiation. The values for the u and d tagging of [16] were averaged.

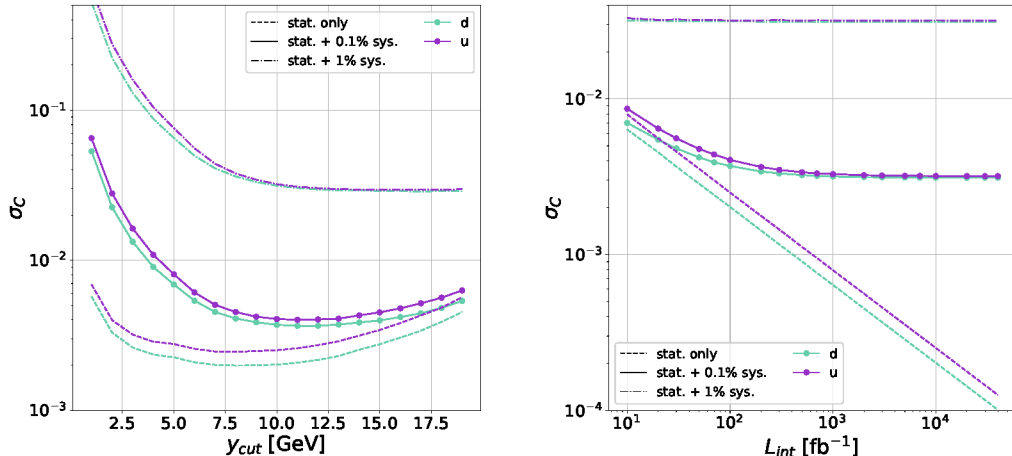


Figure 3. The uncertainty of the d (aquamarine) and u (purple) coupling measurement as a function of y_{cut} (left) and the integrated luminosity (right). Dashed lines indicate statistical uncertainty only, solid lines with points – statistical and systematic uncertainties of 0.1% combined, dash-dotted lines – statistical and systematic uncertainties of 1% combined. The luminosity uncertainty was fixed at 10^{-4} . For the left plot, we assume collecting 100 fb^{-1} of data and for the right plot, we set the value of y_{cut} to 10 GeV.

- relative uncertainty on the integrated luminosity,
- relative uncertainty on the radiative event selection efficiency,
- relative uncertainty on the background to the radiative sample due to photons coming from hadronisation,
- tagging uncertainties (introduced for all tagging and mis-tagging probabilities used in the fit procedure)⁵.

For simplicity, we initially set uncertainties to the same value for all the contributions, except for the luminosity uncertainty which was always kept at 10^{-4} (see e.g. [41–43]). The results are shown in Figure 3, where the relative statistical uncertainties on the u and d quark couplings are compared with the total uncertainties calculated assuming the systematic uncertainty value to be either 0.1% or 1%. The left plot presents the dependence of the results on the y_{cut} parameter; as naively estimated from Figure 2, the optimal value of the parameter corresponds to about 10 GeV, where the FSR-initiated photons start to dominate over photons coming from hadronic decays. The right plot shows the dependence on the integrated luminosity. It is evident that this measurement is systematic-dominated and achieving higher luminosity does not improve the results. In the following, we will discuss potential improvements in the measurement and the impact of particular systematic effects.

⁵Setting them as an absolute shift to the elements of the tagging matrix automatically ensures that the tagging uncertainty for the light quarks is larger than for the heavy quarks, as the corresponding elements of the tagging matrix are smaller and an absolute shift of the same magnitude is more significant.

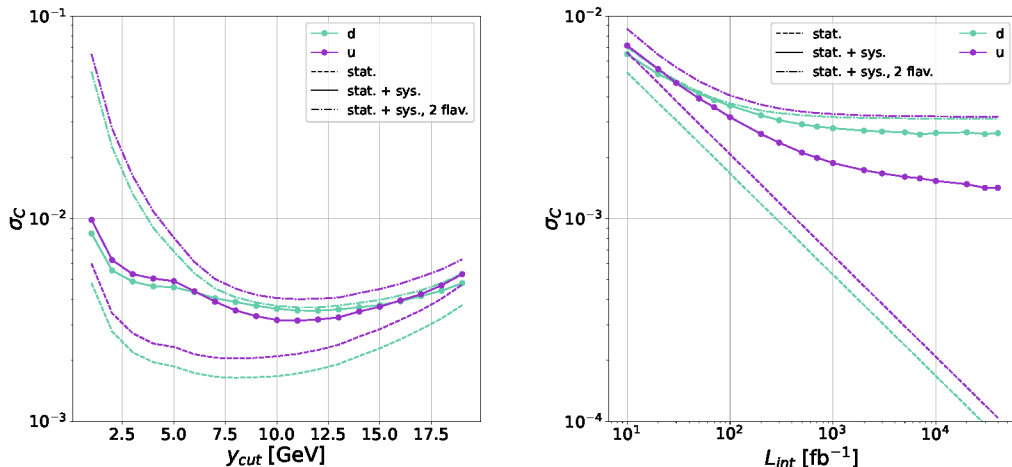


Figure 4. The uncertainty of the d (aquamarine) and u (purple) coupling measurement as a function of y_{cut} (left) and the integrated luminosity (right). Dashed lines indicate statistical uncertainty only, solid lines with points – statistical and systematic uncertainties for the 5-flavour fit, and dash-dotted lines – statistical and systematic uncertainties for the 2-flavour fit. We assume 0.1% uncertainty for all the contributions, except for the luminosity uncertainty (fixed at 10^{-4}). For the left plot, the luminosity was fixed at 100 fb^{-1} and for the right plot, the value of y_{cut} was set to 10 GeV.

4.3 5-flavour fit

To improve our results, we decided to consider the entire data set including all jet flavours. This approach also incorporates events with heavy flavours (e.g. pairs of b jets) and mixed events (e.g. one light jet and one s jet). We hoped to improve the fitting by considering simultaneously all information available, which can constrain some uncertainties directly from the data.

For this purpose, our statistical framework was extended to include all possible jet combinations, and the fitting procedure was repeated. A comparison between the 2- and 5-flavour fits is given in Figure 4. The improvement is especially remarkable for lower values of y_{cut} and large luminosities. As expected, the inclusion of other channels allows for constraining systematic uncertainties from the data, which results in scaling of the measurement uncertainty with growing luminosity. It is also interesting to note that the precision for the d quark becomes worse than for the u quark at larger statistics which can be explained by the signal contamination originating from the s -quark channel.

Figure 5 gives more insight into the results obtained. In the left plot, we show the dependence of the results on y_{cut} for all five flavours. Our statistical framework allows for setting stringent limits for all the quark flavours. In the most favourable case of the b quark, our analysis developed for the light-quark case, can still provide results by a factor of four better than the current measurement. The light-quark couplings could be constrained at the sub-percent level, yielding an essential prospect for the electroweak precision measurements. It is also worth noting that the results for light quarks are significantly worse already at

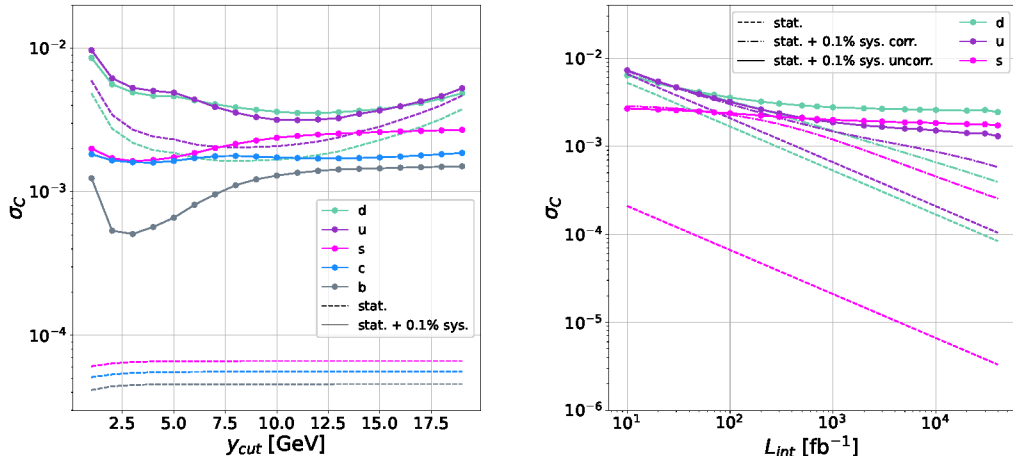


Figure 5. The uncertainty of the d (aquamarine), u (purple), s (pink), c (blue) and b (gray) coupling measurement as a function of y_{cut} (left) and the integrated luminosity (right). Dashed lines indicate statistical uncertainty only, the two other lines – statistical and systematic uncertainties combined for two cases: solid lines with points for u - and d -tagging uncertainties uncorrelated, dash-dotted lines for u - and d -tagging uncertainties fully correlated. We assume 0.1% uncertainty for all the contributions, except for the luminosity (fixed at 10^{-4}). For the left plot, the luminosity was fixed at 100 fb^{-1} and for the right plot, the value of y_{cut} was set to 10 GeV. Data for heavy quarks (correlated u - and d -tagging uncertainties) are skipped in the right (left) plot to improve readability.

the statistical level, which is connected to the number of events tagged into this category.

In the right plot, we present our results as a function of the integrated luminosity for the three lightest quarks. Additionally, we present lines showing the case in which tagging (and mis-tagging) probabilities are assumed to be identical for the two light quarks (their systematic variations are fully correlated), reducing the number of systematic uncertainties considered in the fit. For all the other results presented in this work, we followed the conservative path of assuming that all systematic variations are independent (they are fully uncorrelated). The figure shows that this assumption has a crucial impact on the results. We emphasize that even though the u and d jets are classified into the same category of “light jet”, the uncertainties for the two physical particles are in principle independent.

4.4 Discussion of systematic uncertainties

For the previous considerations, we set all the systematic uncertainties except for the luminosity uncertainty to the same value. However, it is illuminating to loosen this assumption and estimate the impact of particular sources of uncertainty. Figure 6 shows this comparison by varying the uncertainties connected to selection efficiency of radiative events, hadronisation background and tagging, respectively. Three values are considered: 0.1% (treated elsewhere as the “reference” value, and used also for non-varied sources of systematic uncertainties in each plot), 0.01% and 1%. The tagging uncertainty has a crucial impact on

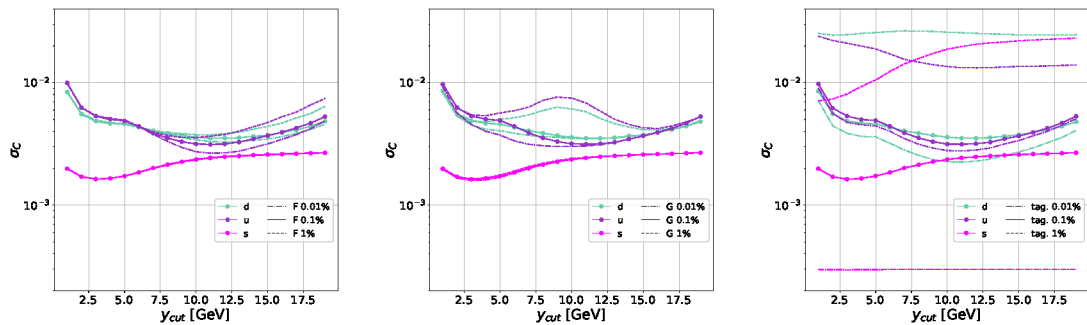


Figure 6. The uncertainty of the d (aquamarine), u (purple) and s (pink) coupling measurement as a function of y_{cut} . The left plot shows the variation of the uncertainty of the acceptance of radiative events, the central one – the uncertainty of the acceptance of non-radiative events, and the right one – the tagging uncertainty. The solid lines indicate the uncertainty of 0.1%, the dashed lines – of 1%, and the dash-dotted ones – of 0.01%. We assume 0.1% uncertainty for all the unvaried contributions, except for the luminosity (fixed at 10^{-4}). The luminosity was set to 100 fb^{-1} .

the results, while the dependence on the uncertainty of the acceptance of hadronic events is rather small and appears only for larger values of y_{cut} . The impact of the uncertainty on the acceptance of radiative events is marginal in the considered range. We stress that to fully explore the physics potential of future Z -pole runs at lepton colliders, a deep understanding of jet tagging is mandatory.

In Figure 7, we show the results as a function of the luminosity for different values of the tagging uncertainty. The plot clearly shows that to benefit from higher data statistics, sub-permille tagging uncertainty must be achieved. According to our study, sub-percent level precision for the light-quark couplings to the Z boson can be achieved at a future experiment collecting 100 fb^{-1} of data, provided that the tagging uncertainty is reduced below 0.3%, and the relative uncertainty on the background to the radiative sample from hadronisation photons remains at 1% or below. The effect of the relative uncertainty on the radiative event selection efficiency is found to be marginal. With higher integrated luminosities, these requirements can be relaxed. For instance, at 40 ab^{-1} , the tagging uncertainty may be allowed up to 0.4%, while the impact of both the radiative event selection efficiency uncertainty and the hadronisation photon background uncertainty becomes negligible.

4.5 Discussion of correlations in the measurement

The measurement aims to disentangle the dependence of the cross sections on the quark couplings, but the measured parameters of the SM are all correlated. By collecting more data of better quality, one can minimise this effect. In Figure 8, we show the correlation ellipses for the d and u quark couplings as their deviation from the SM values. We compare the improvement one can achieve by increasing luminosity or improving tagging efficiency. Both an improvement in the amount of data collected and a higher tagging efficiency change the sensitivity of this measurement and can significantly enhance the precision.

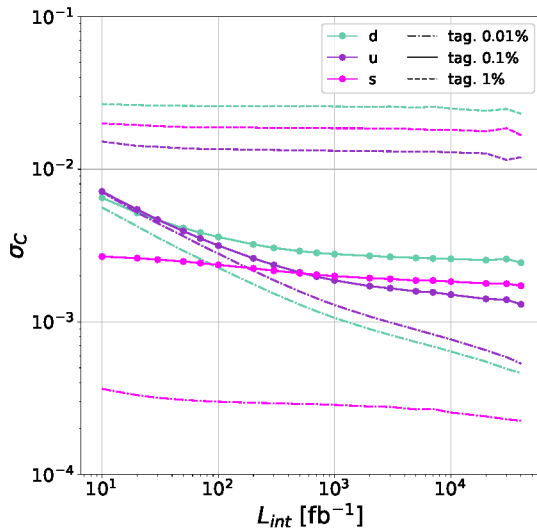


Figure 7. The uncertainty of the d (aquamarine), u (purple) and s (pink) coupling measurement as a function of the integrated luminosity. The plot shows the variation of the tagging uncertainty; the solid lines indicate the uncertainty of 0.1%, the dashed lines – of 1%, and the dash-dotted one – of 0.01%. We assume 0.1% uncertainty for all the unvaried contributions, except for the luminosity (fixed at 10^{-4}). The y_{cut} parameter was set to 10 GeV.

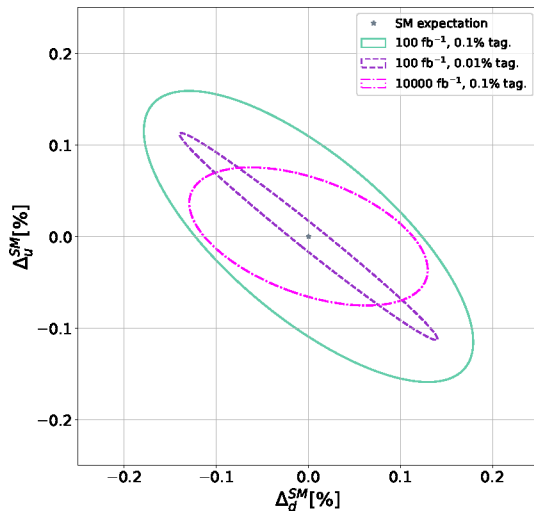


Figure 8. The correlation ellipses for the measurement of the d and u couplings for three different cases: 100 fb^{-1} of collected data with tagging uncertainty of 0.1% (solid aquamarine), 100 fb^{-1} of collected data with tagging uncertainty of 0.01% (dashed purple), 10000 fb^{-1} of collected data with tagging uncertainty of 0.1% (dash-dotted pink), respectively. The deviation from the SM value is shown. We assume 0.1% uncertainty for all the other contributions, except for the luminosity (fixed at 10^{-4}). The y_{cut} parameter was set to 10 GeV.

5 Conclusions and outlook

Future e^+e^- colliders operating at the Z -pole will further constrain the Standard Model parameters and possibly pave the path beyond. Precision measurements of the Z -boson couplings to fermions will be possible thanks to very high data statistics. In this study, we established a dedicated event generation procedure including photons coming from different sources – ISR, FSR, hadronisation and hadron decays. We simulated the detector response and studied photon isolation criteria. Finally, we estimated the expected uncertainties of the measurement of u and d quark couplings to the Z boson, including statistical and systematic contributions. Our study shows that in order to profit from the extremely high luminosities foreseen for future e^+e^- colliders, systematic uncertainties of the tagging efficiency should be brought down to the sub-permille level. High precision should also be secured for theoretical calculations and Monte Carlo simulations affecting the uncertainty of measuring radiative events and misidentifying hadronisation photons. For uncertainties of 0.1%, one can expect a precision of about 0.3% for the measurement of the light-quark couplings to the Z boson, improving upon the statistically limited LEP data by at least an order of magnitude. In general, for integrated luminosities considered for future experiments at e^+e^- colliders, the tagging uncertainty should achieve a precision of 0.3-0.4% to measure the light-quark couplings to the Z bosons at the sub-percent precision. For an integrated luminosity of 100 fb^{-1} , the uncertainty on misidentifying hadronisation photons should be constrained at the level of 1%, while its impact at an integrated luminosity of 40 fb^{-1} becomes negligible. At the same time, our generic framework allows for constraining the precision of the b (c) coupling up to 0.05% (0.1%), which yields an improvement of a factor of 5-20 and can potentially be further optimised. Additional insight could be gained by extending the analysis to higher-energy runs of the future e^+e^- colliders, which has been deferred to future investigations. In order to further disentangle the different vector and axial vector contribution to the Z boson couplings of light quarks polarised beams would be very helpful, though some information could already be gathered by using forward-backward asymmetries at the Z -pole. Such a study is beyond the scope of this work. Moreover, a similar approach of distinguishing between u - and d -type quarks via photon radiation might be used to enhance other precision measurements in hadronic channels, including $H \rightarrow q\bar{q}$ decays.

Acknowledgments

The authors thank the ILD collaboration members for fruitful discussions, valuable comments and suggestions. The work was supported by the National Science Centre (Poland) under OPUS research project no. 2021/43/B/ST2/01778 and the Deutsche Forschungsgemeinschaft (Germany) under Germany's Excellence Strategy-EXC 2121 "Quantum Universe"-390833306. Furthermore, we acknowledge support from the COMETA COST Action CA22130, by EAJADE - Europe- America-Japan Accelerator Development and Exchange Programme (101086276), and from the International Center for Elementary Particle Physics (ICEPP), the University of Tokyo.

A Coupling fit framework

In this Appendix, we review the details of the statistical analysis used for data fitting.

A.1 Fit with statistical uncertainties only

The cross section for each quark flavour can be presented as a sum of processes with and without hard photon radiation (the zero-photon exclusive and one-photon inclusive sample) in the final state:

$$\sigma_q = \sigma_{0q} + \sigma_{\gamma q}, \quad (\text{A.1})$$

where the separation depends on the cuts defined for the photon isolation at the Matrix Element level and in the matching procedure. The resulting fraction of hard radiative events at the generator level is then given by

$$f_q = \frac{\sigma_{\gamma q}}{\sigma_q}. \quad (\text{A.2})$$

The definition of a *radiative* event is imminently connected to photon reconstruction criteria. Thus, one has to define a set of cuts y (including transverse momentum, isolation angle, etc.) describing reconstructable hard photons. Then, the measured radiative cross section depends on the factors $F_y \equiv F(y)$ and $G_y \equiv G(y)$ (assumed to be quark-flavour independent for simplicity) which describe the experimental acceptance of radiative and non-radiative events (for which measurable photons come mostly from hadronisation and decays), respectively:

$$\sigma_{\gamma h}^{(y)} = \sum_q F_y \cdot \sigma_{\gamma q} + G_y \cdot \sigma_{0q} \quad (\text{A.3})$$

$$= \sum_q \sigma_q \cdot (f_q F_y + (1 - f_q) G_y). \quad (\text{A.4})$$

Experimentally, based on the dedicated flavour-tagging algorithms, one can classify hadronic 2-jet-like events into N flavour-based categories. One can classify events assuming same-flavour quark pair production, for example, $b\bar{b}$, $c\bar{c}$ and lighter-quark final states ($N = 3$) or complete flavour decomposition ($b\bar{b}$, $c\bar{c}$, $s\bar{s}$, $u\bar{u}$, $d\bar{d}$, $N = 5$). On the other hand, one can also classify events based on single jet-tagging results (which can differ between the two jets in an event), resulting in more possible event categories (up to $N = 15$ for full flavour decomposition). The advantage of the second approach is that the systematic uncertainties due to flavour-tagging efficiencies can be better constrained from data.

Let j be an index referring to a given flavour category, $j = 1, \dots, N$. The total number of hadronic events expected in each category, after the final selection and classification, can be written as:

$$N_j = \sum_q \mathcal{E}_q \cdot M_{qj} \cdot \mathcal{L}_{int} \cdot \sigma_q, \quad (\text{A.5})$$

where \mathcal{E}_q is the event selection efficiency for flavour q , with results obtained from the simulation in our study are provided in Table 2, \mathcal{L}_{int} is the total integrated luminosity and

q	d	u	s	c	b
\mathcal{E}_q	0.955	0.955	0.947	0.949	0.936
\mathcal{E}_{0q}	0.902	0.903	0.852	0.892	0.870
$\mathcal{E}_{\gamma q}$	0.917	0.922	0.876	0.914	0.888

Table 2. Event selection efficiencies obtained from the simulation. See text for details.

M_{qj} gives the probability of the $q\bar{q}$ event being classified as category j . A similar equation can be set for radiative events:

$$N_{\gamma j}^{(y)} = \sum_q \left(\mathcal{E}_{\gamma q} \cdot M_{\gamma q j} \cdot f_q \cdot F_y + \mathcal{E}_{0q} \cdot M_{0q j} \cdot (1 - f_q) \cdot G_y \right) \cdot \mathcal{L}_{int} \cdot \sigma_q, \quad (\text{A.6})$$

where $\mathcal{E}_{\gamma q}$ and \mathcal{E}_{0q} are the selection efficiencies for radiative events and non-radiative background, i.e. “fake” radiative or category migration events (not taking into account the photon selection cut efficiencies included in F_y and G_y , respectively; Table 2), $M_{\gamma q j}$ and $M_{0q j}$ are the jet-flavour classification matrices for radiative and non-radiative events. In the following, we will assume that $M_{qj} = M_{\gamma q j} = M_{0q j}$. The following tagging-efficiency matrix was adapted from [16]:

$$\begin{bmatrix} 0.773 & 0.190 & 0.031 & 0.006 \\ 0.773 & 0.190 & 0.031 & 0.006 \\ 0.311 & 0.645 & 0.038 & 0.006 \\ 0.107 & 0.068 & 0.795 & 0.030 \\ 0.026 & 0.007 & 0.059 & 0.908 \end{bmatrix}. \quad (\text{A.7})$$

The five rows of the matrix correspond to five quark flavours (d , u , s , c , b), and the four columns to four available jet classification labels (“light jet”, “ s jet”, “ c jet”, “ b jet”). To simplify the formula, we define two matrices:

$$A_{qj} = \mathcal{E}_q \cdot M_{qj} \cdot \mathcal{L}_{int}, \quad (\text{A.8})$$

$$B_{qj} = \mathcal{E}_{\gamma q} \cdot M_{qj} \cdot \mathcal{L}_{int} \cdot f_q \cdot F_y + \mathcal{E}_{0q} \cdot M_{qj} \cdot \mathcal{L}_{int} \cdot (1 - f_q) \cdot G_y \quad (\text{A.9})$$

and we rewrite⁶:

$$N_j = \sum_q A_{qj} \cdot \sigma_q, \quad (\text{A.10})$$

$$N_{\gamma j} = \sum_q B_{qj} \cdot \sigma_q. \quad (\text{A.11})$$

Collider experiments are expected to measure event numbers in $2N$ categories (total hadronic and radiative) and we want to extract $M = 5$ quark-level cross sections which are

⁶We will treat the dependence on y as implicitly assumed and drop the superscript in $N_{\gamma j}^{(y)}$.

directly related to the quark couplings. Assuming the number of events is large for each category j , we consider the χ^2 function:

$$\chi^2 = \sum_j \frac{(n_j - N_j)^2}{n_j} + \sum_j \frac{(n_{\gamma j} - N_{\gamma j})^2}{n_{\gamma j}}, \quad (\text{A.12})$$

where n_j and $n_{\gamma j}$ are the numbers of hadronic and radiative events, respectively, observed in given categories.

Following the maximum likelihood principle, we calculate partial derivatives with respect to σ_q and obtain a system of M equations for cross section values, which can be represented in a matrix form:

$$\mathbb{H} \cdot \vec{\sigma} = \mathbb{V} \quad (\text{A.13})$$

or alternatively ($i = 1, \dots, M$):

$$\sum_q \mathbb{H}_{iq} \cdot \sigma_q = \mathbb{V}_i, \quad (\text{A.14})$$

where the Hessian matrix \mathbb{H} and vector \mathbb{V} are defined as:

$$\mathbb{H}_{iq} = \frac{1}{2} \frac{\partial^2 \chi^2}{\partial \sigma_i \partial \sigma_q} = \sum_j \frac{A_{ij} A_{qj}}{N_j} + \sum_j \frac{B_{ij} B_{qj}}{N_{\gamma j}}, \quad (\text{A.15})$$

$$\mathbb{V}_i = \sum_j \frac{n_j}{N_j} A_{ij} + \sum_j \frac{n_{\gamma j}}{N_{\gamma j}} B_{ij}, \quad (\text{A.16})$$

respectively. The solution can be found by inverting matrix \mathbb{H} :

$$\vec{\sigma} = \mathbb{H}^{-1} \cdot \mathbb{V} \quad (\text{A.17})$$

$$\sigma_i = \sum_q (\mathbb{H}^{-1})_{iq} \mathbb{V}_q. \quad (\text{A.18})$$

The inverse of the Hessian matrix is also the covariance matrix for the extracted cross sections. In particular, cross-section uncertainties are given by the square root of the diagonal elements of the inverse matrix:

$$\Delta \sigma_i = \sqrt{(\mathbb{H}^{-1})_{ii}}. \quad (\text{A.19})$$

Since the cross section linearly depends on the quark coupling, and the proportionality constant can be precisely determined from theoretical calculations, we assume that the uncertainty on the coupling is the same as the uncertainty of the cross-section measurement, $\Delta \sigma_i \equiv \sigma_C$.

A.2 Including systematic uncertainties

The matrices A_{qj} and B_{qj} can be obtained from Monte Carlo simulations of the physics processes and detector performance with negligible statistical uncertainty. However, they are a subject of multiple systematic uncertainties which have to be taken into account.

Assuming K independent systematic uncertainties described by variations δ_k , we can extend the χ^2 formula to include dependence on the systematic variations:

$$\chi^2(\vec{\delta}) = \sum_j \frac{(n_j - N_j(\vec{\delta}))^2}{n_j} + \sum_j \frac{(n_{\gamma j} - N_{\gamma j}(\vec{\delta}))^2}{n_{\gamma j}} + \sum_k \delta_k^2 + \sum_q 2\lambda_q w_q(\vec{\delta}), \quad (\text{A.20})$$

where the third term corresponds to the assumed normal distribution for the systematic variations δ_k and the last term includes Lagrange multipliers λ_q introduced to enforce proper normalisation of the tagging probabilities (the sum of their variations, w_q , has to be zero for each quark flavour q). The dependence of the numbers of expected hadronic and radiative events, N_j and $N_{\gamma j}$, on the considered systematic effects is described by the variation of matrices A_{qj} and B_{qj} (see eqs A.10 and A.11). To allow for a semi-analytical solution, we restrict ourselves to the linear dependence of A_{qj} and B_{qj} on the systematic variations, δ_k , and rewrite:

$$A_{qj} = A_{qj}^{MC} + \sum_k a_{qj}^k \cdot \delta_k, \quad (\text{A.21})$$

$$B_{qj} = B_{qj}^{MC} + \sum_k b_{qj}^k \cdot \delta_k, \quad (\text{A.22})$$

where a_{qj}^k and b_{qj}^k correspond to 1σ variations of A_{qj}^{MC} and B_{qj}^{MC} (which are the nominal values obtained from the Monte Carlo simulation) due to systematic uncertainty k . In the linear approximation, it is also useful to rewrite the experimentally measured cross sections by defining the expected cross section (theoretical value calculated within the SM), σ_q^{th} , and the cross-section deviation parameters, Δ_q :

$$\sigma_q = \sigma_q^{th} + \Delta_q. \quad (\text{A.23})$$

When solving the maximum likelihood problem with systematic uncertainties included, one tries to find a solution for Δ_q , δ_k (and λ_q) assuming small deviations from the nominal predictions, $|\Delta_q| \ll \sigma_q^{th}$, $|a_{qj}^k| \ll A_{qj}$ and $|b_{qj}^k| \ll B_{qj}$, so that terms including products of deviations ($\Delta_q \Delta_{q'}$, $\delta_k \delta_{k'}$ and $\Delta_q \delta_k$) can be neglected. The problem can be reduced to solving the system of $2M + K$ linear equations, similar to the one previously discussed:

$$\tilde{\mathbb{H}} \cdot \begin{pmatrix} \vec{\Delta} \\ \vec{\delta} \\ \vec{\lambda} \end{pmatrix} = \tilde{\mathbb{V}}. \quad (\text{A.24})$$

References

- [1] **European Strategy Group** Collaboration, *2020 Update of the European Strategy for Particle Physics*. CERN Council, Geneva, 2020.
- [2] **P5** Collaboration, S. Asai et al., *Exploring the Quantum Universe: Pathways to Innovation and Discovery in Particle Physics*, [arXiv:2407.19176](#).
- [3] **CEPC Study Group** Collaboration, M. Dong et al., *CEPC Conceptual Design Report: Volume 2 - Physics & Detector*, [arXiv:1811.10545](#).
- [4] **CEPC Study Group** Collaboration, W. Abdallah et al., *CEPC Technical Design Report: Accelerator, Radiat. Detect. Technol. Methods* **8** (2024), no. 1 1–1105, [[arXiv:2312.14363](#)]. [Erratum: *Radiat. Detect. Technol. Methods* **9**, 184–192 (2025)].
- [5] **FCC** Collaboration, A. Abada et al., *FCC Physics Opportunities: Future Circular Collider Conceptual Design Report Volume 1*, *Eur. Phys. J. C* **79** (2019), no. 6 474.
- [6] *The International Linear Collider Technical Design Report - Volume 1: Executive Summary*, [arXiv:1306.6327](#).
- [7] **ILC** Collaboration, *The International Linear Collider Technical Design Report - Volume 2: Physics*, [arXiv:1306.6352](#).
- [8] H. Abramowicz et al., *The International Linear Collider Technical Design Report - Volume 4: Detectors*, [arXiv:1306.6329](#).
- [9] **Linear Collider Vision** Collaboration, C. Balazs et al., *A Linear Collider Vision for the Future of Particle Physics*, [arXiv:2503.19983](#).
- [10] **Linear Collider** Collaboration, H. Abramowicz et al., *The Linear Collider Facility (LCF) at CERN*, [arXiv:2503.24049](#).
- [11] **Particle Data Group** Collaboration, S. Navas et al., *Review of particle physics*, *Phys. Rev. D* **110** (2024), no. 3 030001.
- [12] S. Bilokin, R. Pöschl, and F. Richard, *Measurement of b quark EW couplings at ILC*, [arXiv:1709.04289](#).
- [13] J. Fuster, A. Irlles, G. Rodrigo, S. Tairafune, M. Vos, H. Yamamoto, and R. Yonamine, *Prospects for the measurement of the b -quark mass at the ILC*, in *International Workshop on Future Linear Colliders*, **4**, 2021. [arXiv:2104.09924](#).
- [14] A. Irlles, R. Pöschl, and F. Richard, *Experimental methods and prospects on the measurement of electroweak b and c -quark observables at the ILC operating at 250 GeV*, [arXiv:2306.11413](#).
- [15] R. Tagami, T. Suehara, and M. Ishino, *Application of Particle Transformer to quark flavor tagging in the ILC project*, *EPJ Web Conf.* **315** (2024) 03011, [[arXiv:2410.11322](#)].
- [16] H. Liang, Y. Zhu, Y. Wang, Y. Che, C. Zhou, H. Qu, and M. Ruan, *Jet-Origin Identification and Its Application at an Electron-Positron Higgs Factory*, *Phys. Rev. Lett.* **132** (2024), no. 22 221802, [[arXiv:2310.03440](#)].
- [17] Y. Zhu, H. Liang, Y. Wang, H. Qu, C. Zhou, and M. Ruan, *ParticleNet and its application on CEPC jet flavor tagging*, *Eur. Phys. J. C* **84** (2024), no. 2 152, [[arXiv:2309.13231](#)].
- [18] F. Blekman, F. Canelli, A. De Moor, K. Gautam, A. Ilg, A. Macchiolo, and E. Ploerer,

Tagging more quark jet flavours at FCC-ee at 91 GeV with a transformer-based neural network, *Eur. Phys. J. C* **85** (2025), no. 2 165, [[arXiv:2406.08590](#)].

- [19] A. Albert et al., *Strange quark as a probe for new physics in the Higgs sector*, in *Snowmass 2021*, 3, 2022. [[arXiv:2203.07535](#)].
- [20] **DELPHI** Collaboration, P. Abreu et al., *Study of final state photons in hadronic Z0 decay and limits on new phenomena*, *Z. Phys. C* **53** (1992) 555–566.
- [21] **L3** Collaboration, O. Adriani et al., *Isolated hard photon emission in hadronic Z0 decays*, *Phys. Lett. B* **292** (1992) 472–484.
- [22] **L3** Collaboration, O. Adriani et al., *Determination of quark electroweak couplings from direct photon production in hadronic Z decays*, *Phys. Lett. B* **301** (1993) 136–144.
- [23] **DELPHI** Collaboration, P. Abreu et al., *Study of prompt photon production in hadronic Z0 decays*, *Z. Phys. C* **69** (1995) 1–14.
- [24] **OPAL** Collaboration, G. Abbiendi et al., *Measurement of the partial widths of the Z into up and down type quarks*, *Phys. Lett. B* **586** (2004) 167–182, [[hep-ex/0312043](#)].
- [25] A. Robson and C. Leonidopoulos, *The ECFA Higgs/Electroweak/Top Factory Study*, tech. rep., 2024.
- [26] J. Kalinowski, W. Kotlarski, P. Sopicki, and A. F. Zarnecki, *Simulating hard photon production with WHIZARD*, *Eur. Phys. J. C* **80** (2020), no. 7 634, [[arXiv:2004.14486](#)].
- [27] W. Kilian, T. Ohl, and J. Reuter, *Whizard—simulating multi-particle processes at lhc and ilc*, *The European Physical Journal C* **71** (Sept., 2011).
- [28] M. Moretti, T. Ohl, and J. Reuter, *O’mega: An optimizing matrix element generator*, 2001.
- [29] W. Kilian, T. Ohl, J. Reuter, and C. Speckner, *QCD in the Color-Flow Representation*, *JHEP* **10** (2012) 022, [[arXiv:1206.3700](#)].
- [30] P. M. Brecht, W. Kilian, J. Reuter, and P. Stienemeier, *NLO electroweak corrections to multi-boson processes at a muon collider*, *JHEP* **12** (2022) 138, [[arXiv:2208.09438](#)].
- [31] S. Brass, W. Kilian, and J. Reuter, *Parallel Adaptive Monte Carlo Integration with the Event Generator WHIZARD*, *Eur. Phys. J. C* **79** (2019), no. 4 344, [[arXiv:1811.09711](#)].
- [32] B. Chokoufe Nejad, T. Ohl, and J. Reuter, *Simple, parallel virtual machines for extreme computations*, *Comput. Phys. Commun.* **196** (2015) 58–69, [[arXiv:1411.3834](#)].
- [33] S. Jadach, B. F. L. Ward, and Z. Was, *The Precision Monte Carlo event generator KK for two fermion final states in e+ e- collisions*, *Comput. Phys. Commun.* **130** (2000) 260–325, [[hep-ph/9912214](#)].
- [34] S. Jadach, B. F. L. Ward, and Z. Was, *KK MC 4.22: Coherent exclusive exponentiation of electroweak corrections for $f\bar{f} \rightarrow f'\bar{f}'$ at the LHC and muon colliders*, *Phys. Rev. D* **88** (2013), no. 11 114022, [[arXiv:1307.4037](#)].
- [35] T. Sjostrand, S. Mrenna, and P. Z. Skands, *PYTHIA 6.4 Physics and Manual*, *JHEP* **05** (2006) 026, [[hep-ph/0603175](#)].
- [36] T. Sjöstrand, S. Ask, J. R. Christiansen, R. Corke, N. Desai, P. Ilten, S. Mrenna, S. Prestel, C. O. Rasmussen, and P. Z. Skands, *An introduction to PYTHIA 8.2*, *Comput. Phys. Commun.* **191** (2015) 159–177, [[arXiv:1410.3012](#)].

- [37] **DELPHES 3** Collaboration, J. de Favereau et al., *DELPHES 3, A modular framework for fast simulation of a generic collider experiment*, *JHEP* **02** (2014) 057, [[arXiv:1307.6346](#)].
- [38] **ILD Concept Group** Collaboration, H. Abramowicz et al., *International Large Detector: Interim Design Report*, [arXiv:2003.01116](#).
- [39] **SiD Consortium** Collaboration, A. P. White, *The SiD Detector for the International Linear Collider*, in *Meeting of the APS Division of Particles and Fields*, 10, 2015. [arXiv:1511.00134](#).
- [40] **ILD** Collaboration, U. Einhaus, *The International Large Detector (ILD) for a future electron-positron collider: Status and Plans*, *PoS EPS-HEP2023* (2024) 543, [[arXiv:2311.09181](#)].
- [41] I. Božović Jelisavčić, S. Lukić, G. Milutinović Dumbelović, M. Pandurović, and I. Smiljanić, *Luminosity measurement at ILC*, *JINST* **8** (2013) P08012, [[arXiv:1304.4082](#)].
- [42] S. Jadach, W. Płaczek, M. Skrzypek, B. F. L. Ward, and S. A. Yost, *The path to 0.01% theoretical luminosity precision for the FCC-ee*, *Phys. Lett. B* **790** (2019) 314–321, [[arXiv:1812.01004](#)].
- [43] M. Dam, *Challenges for FCC-ee luminosity monitor design*, *Eur. Phys. J. Plus* **137** (2022), no. 1 81, [[arXiv:2107.12837](#)].